Electrical Power and Energy Systems 55 (2014) 497–502

Contents lists available at ScienceDirect

Electrical Power and Energy Systems

journal homepage: www.elsevier.com/locate/ijepes

An energy differential relay for long transmission lines

Minghao Wen *, Deshu Chen, Xianggen Yin

State Key Laboratory of Advanced Electromagnetic Engineering and Technology (Huazhong University of Science and Technology), Hubei, China

ARTICLE INFO

Article history:
Received 12 June 2013
Received in revised form 9 September 2013
Accepted 24 September 2013

Keywords:
Capacitive current
Long transmission line
Line protection
Energy differential relay

ABSTRACT

The operating speed and sensitivity of the current differential protection must be lowered in order to deal with the problems caused by the capacitive currents of the long transmission line. To solve this problem, a new energy differential relay is put forward. The proposed scheme can distinguish between internal and external faults by comparing the energies of two methods. The first method is to calculate the energy flow in the line in a short time interval. The second method is to calculate the energy consumption of distributed elements on the transmission line with the assumption that there is no internal fault on the line. Special means are adopted: use of modal quantities of voltage and current; the instantaneous voltage and current are distributed linearly along the transmission line; the instantaneous voltage and current vary linearly during a sampling interval; the sampling interval is equal to the travel time of the protected line. Thus the energies can be calculated by using the sampled values at each end of the transmission line. It has been proven that the calculated energies of the two different methods are equal when there is no internal fault on the transmission line. The performance of the proposed method has been verified by EMTP simulation tests, dynamic simulation tests and the comparison with a competitive method.

1. Introduction

It is a well recognized fact that differential protection schemes provide sensitive protection with crisp demarcation of the protection zones [1–5]. The voltage level of long-distance transmission lines is usually up to 500-kV or higher. The corresponding protection must trip as rapidly as possible to mitigate the damage if an internal fault occurs within this line. However, the line charging current component is significant and it causes a large variation in phase angle of the line current from one end to another. In traditional current differential schemes, relaying sensitivity will have to be compromised to prevent the mal-operation. Among existing technologies dealing with the impacts of the distributed capacitive current, most of them employ a higher operating threshold of the differential protection. Besides, some capacitive current compensation algorithms are employed for the phasor based differential protection [6–8]. In this case, the sensitivity and the operation speed will be lowered. Ref. [9] proposed a current differential relay which uses distributed line model to consider line charging current. An adaptive GPS-synchronized protection scheme using Clarke transformation has been proposed in [10]. A transmission line pilot protection scheme based on the individual phase impedance has been proposed in [11]. An adaptive restraint coefficient-based differential protection criterion was introduced [12]. In [13], the dynamic behavior of the power differential relay has been thoroughly investigated.

A new technique for long transmission line protection is put forward. The proposed scheme can distinguish between internal and external faults by comparing the results of the net energy fed into the protected line in a short time interval. The energy is calculated by two different methods. The first method is to calculate the energy flow in the line in a short time interval. The second method is to calculate the energy consumption of distributed elements on the transmission line with the assumption that there is no internal fault on the line. Special means are adopted: 1. use of modal quantities of voltage and current; 2. the instantaneous voltage and current are distributed linearly along the transmission line; 3. the instantaneous voltage and current vary linearly during a sampling interval; and 4. the sampling interval is equal to the travel time of the protected line. The energies of the two methods are equal when there is no internal fault on the transmission line (as proven in Appendix A). The test results show that the proposed technique has highly reliability, fast speed, and excellent performance under high-resistance earth-fault conditions.

This paper is organized as follows: Section 2 enunciates the fundamentals of the proposed scheme. Section 3 presents the algorithms and criteria. Test results are presented in Section 4. Section 5 concludes the paper.

* Corresponding author. Tel./fax: +86 2787540945.
E-mail addresses: swenmh@mail.hust.edu.cn (M. Wen), dschen@mail.hust.edu.cn (D. Chen), xgyin@mail.hust.edu.cn (X. Yin).

0142-0615/$ - see front matter © 2013 Elsevier Ltd. All rights reserved.
http://dx.doi.org/10.1016/j.ijepes.2013.09.035

2. Fundamentals

The new differential protection scheme is initially explained using a single-phase system in this section. Two different methods are applied to calculate the net energy fed into the protected line during a short time interval. In the 1st method, the voltage and current at each end of the transmission line are used to calculate the instantaneous power. The sum of the power at each end is the instantaneous power flow in the transmission line. Then the energy flow in the transmission line (shown in Fig. 1) from time t_1 to t_2 can be obtained by the integral of the instantaneous power over this interval as given below:

$$E_1 = \int_{t_1}^{t_2} [v_M(t) \cdot i_M(t) - v_N(t) \cdot i_N(t)]dt \tag{1}$$

where $v_M(t)$ is the voltage at the relay point M; $i_M(t)$ the current at the relay point M; $v_N(t)$ the voltage at the relay point N and $i_N(t)$ is the current at the relay point N.

This is the first method to calculate the energy flow in a line in a short time interval. The second method is to calculate the energy consumption of distributed elements on the transmission line with the assumption that there is no internal fault on the line, that is

$$E_2 = \int_{t_1}^{t_2} \times \int_0^l \left(i^2(x,t) \cdot R_0 + i(x,t) \cdot \frac{di(x,t)}{dt} \cdot L_0 + v(x,t) \cdot \frac{dv(x,t)}{dt} \cdot C_0 \right) dxdt \tag{2}$$

where x is the distance from the point X to the relay point M; $v(x, t)$ the voltage at point X; $i(x, t)$ the current at point X; l the total length of the line and R_0, L_0 and C_0 is the resistance, inductance and capacitance of the line per unit length.

The energy consumption is the sum of the energy consumed by the resistance, inductance and capacitance of the line. Based on the voltage and current distributions along the line and the instantaneous voltages and currents during the interval, the energy is calculated by integration.

This technique is based on the energy conservation law; "Energy in a system may neither be created nor destroyed, just converted from one form to another". E_1 is compared with E_2. While there is no internal fault on the line, we have $E_1 = E_2$. If there are some differences between the two energies, an internal fault is indicated in the transmission line zone.

3. Energy differential relay

The calculation of the energy fed into the protected line (shown in Fig. 1) required the voltage and current distributions along the line and the instantaneous voltages and currents during the interval. Special means are adopted: 1. use of modal quantities of voltage and current; 2. the instantaneous voltage and current are distributed linearly along the transmission line; 3. the instantaneous voltage and current vary linearly during a sampling interval; 4. the sampling interval is equal to the travel time of the protected line.

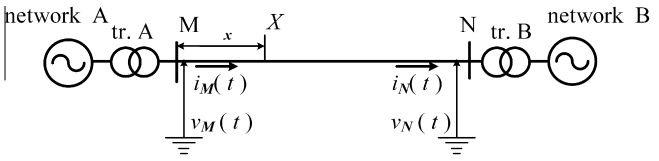

Fig. 1. Circuit diagram of a typical transmission line.

3.1. Algorithm

Assume that the two ends of the protected line are denoted by M and N, the implementation of the protection requires two groups of the space modulus: Modulus 1: v_{MA}–v_{MB}, i_{MA}–i_{MB}, v_{NA}–v_{NB}, i_{NA}–i_{NB}; modulus 2: v_{MA}–v_{MC}, i_{MA}–i_{MC}, v_{NA}–v_{NC}, i_{NA}–i_{NC}. Among which, v_{MA}–v_{MB} represents the voltage difference between phase A and phase B on M side, and i_{NA}–i_{NB} represents the current difference between the phase A and phase B on the N side, and so forth.

Under the assumption that the instantaneous voltage and current are distributed linearly along the transmission line, Eqs. (3) and (4) are derived:

$$v_{m1}(x,t) = v_{Mm1}(t) + \frac{(v_{Nm1}(t) - v_{Mm1}(t))}{l} \cdot x \tag{3}$$

$$i_{m1}(x,t) = i_{Mm1}(t) + \frac{(i_{Nm1}(t) - i_{Mm1}(t))}{l} \cdot x \tag{4}$$

where $v_{m1}(x, t)$ is the voltage of modulus 1 at point X; $v_{Mm1}(t)$ the voltage of modulus 1 on M side; $v_{Nm1}(t)$ the voltage of modulus 1 on N side; $i_{m1}(x, t)$ the current of modulus 1 at point X; $i_{Mm1}(t)$ the current of modulus 1 on M side and $i_{Nm1}(t)$ the current of modulus 1 on N side.

Under the assumption that the instantaneous voltage and current vary linearly during a sampling interval, Eqs. (5)–(8) are derived:

$$v_{Mm1}(t) = v_{Mm1}(k-1) + \frac{v_{Mm1}(k) - v_{Mm1}(k-1)}{\tau} \cdot (t - t_0 - (k-1)\tau) \tag{5}$$

$$v_{Nm1}(t) = v_{Nm1}(k-1) + \frac{v_{Nm1}(k) - v_{Nm1}(k-1)}{\tau} \cdot (t - t_0 - (k-1)\tau) \tag{6}$$

$$i_{Mm1}(t) = i_{Mm1}(k-1) + \frac{i_{Mm1}(k) - i_{Mm1}(k-1)}{\tau} \cdot (t - t_0 - (k-1)\tau) \tag{7}$$

$$i_{Nm1}(t) = i_{Nm1}(k-1) + \frac{i_{Nm1}(k) - i_{Nm1}(k-1)}{\tau} \cdot (t - t_0 - (k-1)\tau) \tag{8}$$

where t_0 is the sampling start time; $v_{Mm1}(k)$, $i_{Mm1}(k)$ the voltage and current sampled value of modulus 1 on M side at sample k; $v_{Nm1}(k)$, $i_{Nm1}(k)$ the voltage and current sampled value of modulus 1 on N side at sample k; $v_{Mm1}(k-1)$, $i_{Mm1}(k-1)$, $v_{Nm1}(k-1)$ and $i_{Nm1}(k-1)$ the voltage and current sampled value of modulus 1 at sample $k-1$ and τ the sampling interval.

The sampling interval is equal to the travel time of the protected line, that is:

$$\tau = l \cdot \sqrt{L_{m1} \cdot C_{m1}} = l \cdot \sqrt{L_{m2} \cdot C_{m2}} \tag{9}$$

where L_{m1}, C_{m1} is the inductance and capacitance of modulus 1 per unit length and L_{m2}, C_{m2} is the inductance and capacitance of modulus 2 per unit length.

Using the 1st method, the energy of modulus 1 flow in the transmission line from time $t_0 + (k-1)\tau$ to $t_0 + k\tau$ can be obtained by the integral of the instantaneous power over this interval between sample $k-1$ and sample k as given below:

$$E_{1m1}(k) = \int_{t_0+(k-1)\tau}^{t_0+k\tau} [v_{Mm1}(t) \cdot i_{Mm1}(t) - v_{Nm1}(t) \cdot i_{Nm1}(t)]dt \tag{10}$$

Using the 2nd method, with the assumption that there is no internal fault on the line, the energy consumption of modulus 1 of the transmission line from time $t_0 + (k-1)\tau$ to $t_0 + k\tau$ can be obtained:

$$E_{2m1}(k) = \int_{t_0+(k-1)\tau}^{t_0+k\tau} \int_0^l \left(i_{m1}^2(x,t) \cdot R_{m1} + i_{m1}(x,t) \cdot \frac{di_{m1}(x,t)}{dt} \cdot L_{m1} + u_{m1}(x,t) \cdot \frac{dv_{m1}(x,t)}{dt} \cdot C_{m1} \right) dxdt \tag{11}$$

where R_{m1} is the resistance of modulus 1 per unit length.

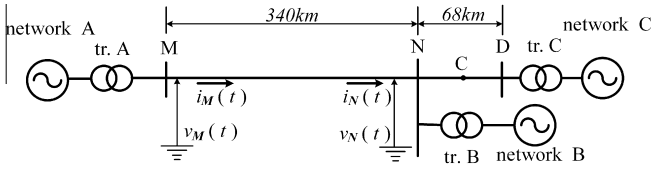

Fig. 2. The schematic diagram of simulation system.

Substituting (5)–(8) into (10), $E_{1m1}(k)$ can be calculated. Substituting (3)–(8) into (11), $E_{2m1}(k)$ can be calculated. Then the energy of modulus 1 flow in the transmission line over the interval between sample p to q is calculated:

$$E_{1m1} = \sum_{k=p}^{k=q} E_{1m1}(k) \tag{12}$$

The energy consumption of modulus 1 of the transmission line over the interval between sample p and sample q is calculated:

$$E_{2m1} = \sum_{k=p}^{k=q} E_{2m1}(k) \tag{13}$$

The energies of the two methods are equal when there is no internal fault on the transmission line (as proven in Appendix A). Similarly, the energy of modulus 2 can be calculated.

3.2. Criterion

The criterion of the modulus 1 energy is independent of the criterion of the modulus 2. By taking the energy of modulus 1 as an illustration, the protection criteria at each sampling time are given by

$$|E_{1m1} - E_{2m1}| > \lambda \cdot E_{\max} \quad \text{And} \quad E_{\max} > E_0 \tag{14}$$

where $E_{\max}$ is the larger of $|E_{1m1}|$ or $|E_{2m1}|$; E_0 the energy threshold according to the error and λ is the restraint factor.

E_{1m1} and E_{2m1} in (14) are calculated according to (12) and (13), in which sample p is the first sample after a fault and sample p is the postfault current sample.

The initial value of the counter trip_counter = 0. If the postfault calculated energy at a sampling time satisfy (14), trip_counter = trip_counter + 1.

The protection will trip if (15) or (16) is true.

$$(p-q)\cdot\tau < 0.5T \quad \text{And} \quad \text{trip\_counter} > k_{set}\cdot\frac{T}{2\tau} \tag{15}$$

$$(p-q)\cdot\tau > 0.5T \quad \text{And} \quad \text{trip\_counter} > k_{set}\cdot(p-q) \tag{16}$$

where T is the one cycle of power frequency and k_{set} the action factor.

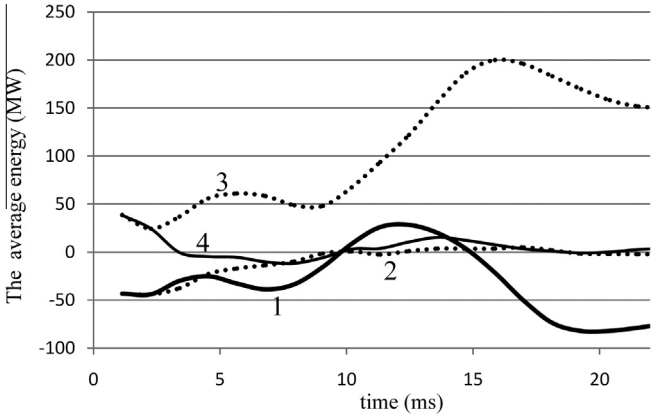

Fig. 3. The average energies for an internal single phase ground fault at 102 km from the bus M. Curve 1: $\frac{E_{1m1}}{(q-p)\cdot\tau}$; curve 2: $\frac{E_{2m1}}{(q-p)\cdot\tau}$; curve 3: $\frac{E_{1m2}}{(q-p)\cdot\tau}$; curve 4: $\frac{E_{2m2}}{(q-p)\cdot\tau}$.

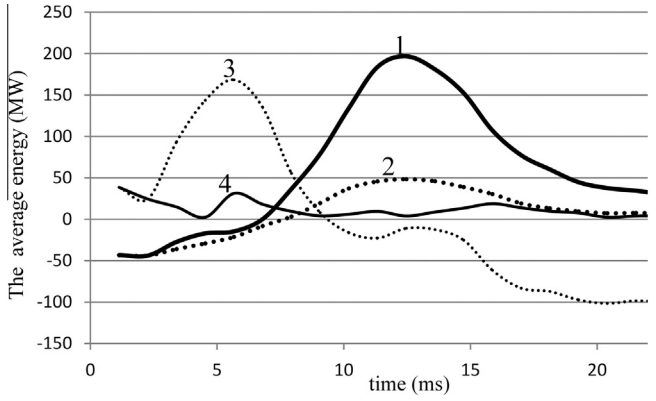

Fig. 4. The average energies for an internal three-phase fault at 102 km from the bus M. Curve 1: $\frac{E_{1m1}}{(q-p)\cdot\tau}$; curve 2: $\frac{E_{2m1}}{(q-p)\cdot\tau}$; curve 3: $\frac{E_{1m2}}{(q-p)\cdot\tau}$; curve 4: $\frac{E_{2m2}}{(q-p)\cdot\tau}$.

4. Test results

4.1. Simulation analysis

The tests have been done based on Electromagnetic Transients Program (EMTP). The schematic diagram of the 500 kV power system is shown in Fig. 2. The electrical parameters are given in Table 1. Line MN is the protected line.

The proposed algorithm was tested with varying fault types, fault distance, fault resistance and phase angle between networks. The sampling rate is set as 882.35 Hz in the case of 50 Hz power frequency. The energy curves calculated by the proposed algorithm are respectively shown in Figs. 3–7. The horizontal axis in these figures represents the current sample time. Here, the fault occurrence is taken as the initial moment. The longitudinal axis stands for the average energies, that is: $\frac{E_{1m1}}{(q-p)\cdot\tau}$, $\frac{E_{2m1}}{(q-p)\cdot\tau}$, $\frac{E_{1m2}}{(q-p)\cdot\tau}$ and $\frac{E_{2m2}}{(q-p)\cdot\tau}$. E_{1m1}, E_{2m1}, E_{1m2} and E_{2m2} are calculated by using Eqs. (10)–(13).

Table 1
The electrical parameters.

	Length (km)	r_1 (Ω/km)	x_1 (Ω/km)	c_1 (nF/km)	r_0 (Ω/km)	x_0 (Ω/km)	c_0 (nF/km)
Line MN	340	0.027	0.28	12.7	0.195	0.649	8.98
Line ND	68	0.027	0.28	12.7	0.195	0.649	8.98
	R_1 (Ω)	L_1 (H)	R_0 (Ω)	L_0 (H)	Equivalent electromotive forces (kV)		
Network A	0.423	0.106	0.187	0.0357	500		
Network B	0.634	0.160	0.280	0.0535	525		
Network C	0.423	0.106	0.187	0.0357	525		

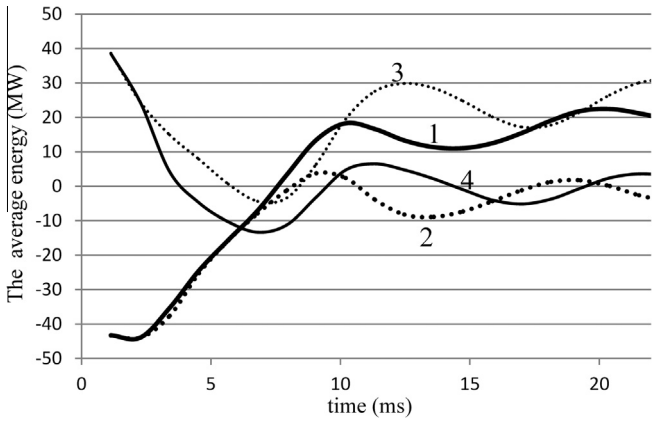

Fig. 5. The average energies for an internal single phase ground fault with 600 Ω fault resistance at 102 km from the bus M. Curve 1: $\frac{E_{1m1}}{(q-p)\cdot\tau}$; curve 2: $\frac{E_{2m1}}{(q-p)\cdot\tau}$; curve 3: $\frac{E_{1m2}}{(q-p)\cdot\tau}$; curve 4: $\frac{E_{2m2}}{(q-p)\cdot\tau}$.

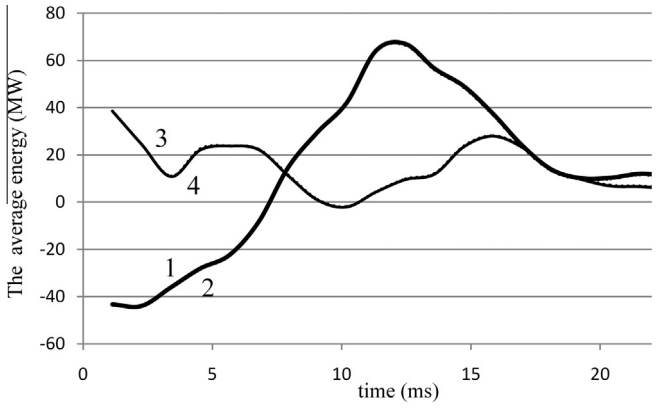

Fig. 6. The average energies for an external three-phase fault at point C. Curve 1: $\frac{E_{1m1}}{(q-p)\cdot\tau}$; curve 2: $\frac{E_{2m1}}{(q-p)\cdot\tau}$; curve 3: $\frac{E_{1m2}}{(q-p)\cdot\tau}$; curve 4: $\frac{E_{2m2}}{(q-p)\cdot\tau}$.

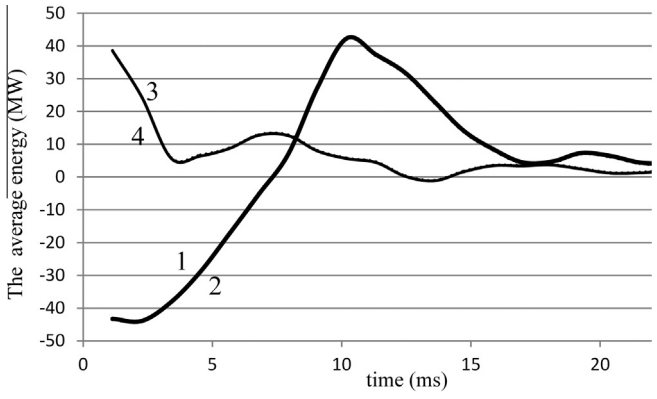

Fig. 7. The average energies for an external double phase-ground fault at point C. Curve 1: $\frac{E_{1m1}}{(q-p)\cdot\tau}$; curve 2: $\frac{E_{2m1}}{(q-p)\cdot\tau}$; curve 3: $\frac{E_{1m2}}{(q-p)\cdot\tau}$; curve 4: $\frac{E_{2m2}}{(q-p)\cdot\tau}$.

Four energy measurement curves are shown in Fig. 3 for a single phase ground fault at 102 km from the bus M. Fig. 4 shows the average energies for a three-phase fault at 102 km from the bus M. Fig. 5 shows the average energies for a single phase ground fault with 600 Ω fault resistance at 102 km from the bus M. It can be observed from Figs. 3–5 that the difference between the energy of modulus 1 calculated by the 1st method (curve 1) and the energy of modulus 1 calculated by the 2nd method (curve 2) is pronounced. The difference between the modulus 2 curves of two methods (curve 3 and curve 4) is also obvious. Therefore, the protection using the new algorithm is able to issue the tripping command rapidly and sensitively.

Table 2
Part of typical results of EMTP simulation tests.

Fault type		ph–G				ph–ph	ph–ph–G	3 ph
Fault position		Fault resistance (Ω)						
		0	90	300	600			
		Operating time (ms)						
Internal	0	5.7	5.7	8.0	8.0	5.7	5.7	5.7
	20	6.9	6.9	6.9	8.0	9.1	9.1	6.9
	40	5.7	5.7	6.9	8.0	5.7	5.7	5.7
	60	5.7	6.9	6.9	8.0	5.7	5.7	5.7
	80	5.7	5.7	6.9	6.9	5.7	5.7	5.7
	100	5.7	5.7	5.7	6.9	5.7	5.7	5.7
External	M	NO	NO	NO	NO	NO	NO	NO
	N	NO	NO	NO	NO	NO	NO	NO
	C	NO	NO	NO	NO	NO	NO	NO
	D	NO	NO	NO	NO	NO	NO	NO

Where, "ph–G" means a single phase to ground fault, "ph–ph" means phase-phase fault. "ph–ph–G" means double phase to ground fault. 3ph means three phase short-circuited fault, and so forth. Besides, NO means no operation.

Fig. 6 shows the average energies for an external three-phase fault at point C (34 km from the bus N). Fig. 7 shows the average energies for an external double phase-ground fault at point C. It can be seen from Figs. 6 and 7 that the energy of modulus 1 calculated by the 1st method (curve 1) coincides with the energy of modulus 1 calculated by the 2nd method (curve 2). The modulus 2 curves of two methods are also almost identical. The results show that the protection for long-distance transmission lines implemented with the new algorithm keeps stable on the occurrence of external faults.

The operating behavior analysis on the new method responding to part of fault scenarios, including various fault types, various fault positions on the occasion of internal faults {0, 20, 40, 60, 80, 100}%, various fault positions on the occasion of external faults {M, N, C, D}, various fault resistance {0, 90, 300, 600} Ω, is outlined in Table 2. Furthermore, a variety of EMTP simulation tests show that, for most internal faults, including the fault with high resistance, the operating times of the new protection are around 5–10 ms.

4.2. Dynamic simulation test

The performance of the energy differential relay is demonstrated by a dynamic simulation test whose model is a 1000-kV 645 km ultra-high-voltage (UHV) line model shown in Fig. 8. The parameters of the protected line from Nanyang switching station to Jingmen side are $D = 285$ km, $r_1 = 0.0068$ Ω/km, $x_1 = 0.267$ Ω/km, $c_1 = 14.0$ nF/km, $r_0 = 0.149$ Ω/km, $x_0 = 0.821$ Ω/km and $c_0 = 9.31$ nF/km. Nanyang switching station is 360 km away from Jindongnan side. Data for Shanxi 500-kV System are: $L_1 = 0.031$ H (min), 0.168 H (max); $L_0 = 0.049$ H (min), 0.205 H (max). Data for Hubei 500-kV System are: $L_1 = 0.029$ H (min), 0.038 H (max); $L_0 = 0.058$ H (min), 0.074 H (max).

The performance of the proposed technique is tested under a variety of fault conditions. The fault cases are described as follows:

- fault location: internal faults {0, 63, 74, 84, 100}%, external faults {B, D, M, N, C, Z};
- fault types: A–G, B–C, B–C–G, and A–B–C–G;
- fault resistance: 0 Ω and 600 Ω;
- prefault load flow: power angle is set as 10, 15, and 20, respectively.

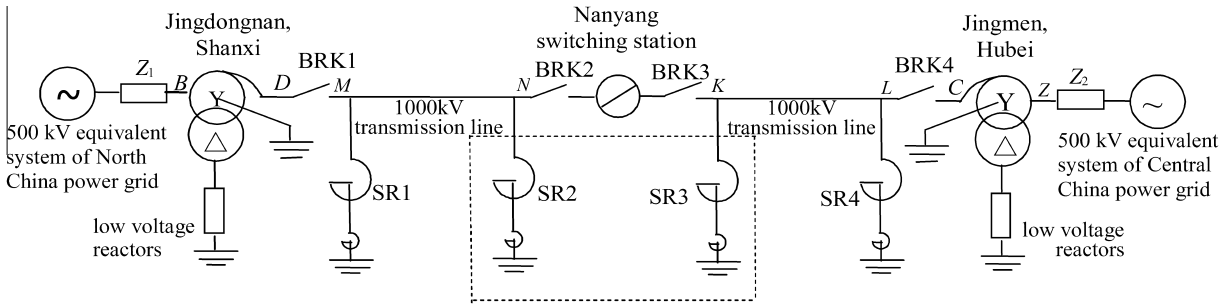

Fig. 8. Ultra-high voltage transmission system.

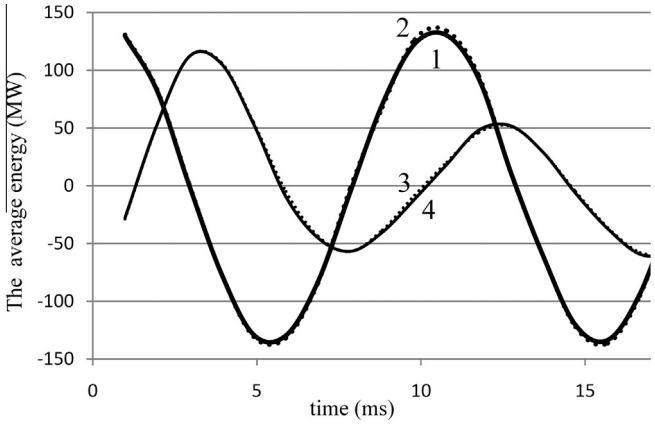

Fig. 9. The average energies for an external single phase ground fault at the bus N. Curve 1: $\frac{E_{1m1}}{(q-p)\cdot\tau}$; curve 2: $\frac{E_{2m1}}{(q-p)\cdot\tau}$; curve 3: $\frac{E_{1m2}}{(q-p)\cdot\tau}$; curve 4: $\frac{E_{2m2}}{(q-p)\cdot\tau}$.

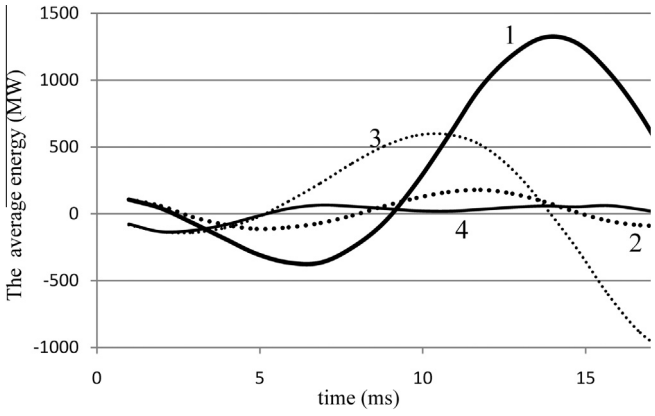

Fig. 10. The average energies for an internal single phase ground fault at 180 km from the bus K. Curve 1:$\frac{E_{1m1}}{(q-p)\cdot\tau}$; curve 2: $\frac{E_{2m1}}{(q-p)\cdot\tau}$; curve 3: $\frac{E_{1m2}}{(q-p)\cdot\tau}$; curve 4: $\frac{E_{2m2}}{(q-p)\cdot\tau}$.

The dynamic simulation test results validated the proposed technique and insured its compatibility and efficacy. Fig. 9 shows the average energies for an external single phase ground fault at the bus N. Fig. 10 shows the average energies for an internal single phase ground fault at 180 km from the bus K. Table 3 provides part of typical results of dynamic simulation tests.

4.3. Comparison with a competitive method

For the purpose of comparison, simulation tests are also made on an adaptive restraint coefficient-based differential protection criterion [12]. The tests have been done based on EMTP. To simplify the description, the criterion in [12] is called as adaptive phasor based differential criterion in the following.

Table 3
Part of typical results of dynamic simulation tests.

Fault type		ph–G		ph–ph	ph–ph–G	3 ph
Fault position		Fault resistance (Ω)				
		0	600			
		Operating time (ms)				
Internal	0	6.9	9.8	8.8	9.8	5.9
	63	6.9	10.8	8.8	8.8	5.9
	74	6.9	8.8	9.8	8.8	7.8
	84	6.9	10.8	9.8	10.8	5.9
	100	5.9	/	10.8	8.8	6.9
External	B	NO	NO	NO	NO	NO
	D	NO	NO	NO	NO	NO
	M	NO	NO	NO	NO	NO
	N	NO	NO	NO	NO	NO
	C	NO	NO	NO	NO	NO
	Z	NO	NO	NO	NO	NO

"/": The dynamic simulation test did not include this fault case.

The simulation results show that the typical operating time of the adaptive phasor based differential protection is 20 ms. Besides, its ability resistive to fault resistance is relatively worse. It may fail-to-trip if the fault resistance is up to 400 Ω. The peak values of the differential currents through faulty phases during external three-phase short-circuit fault may be greater than 500 A. In contrast, the operating times of the new protection are around 5–10 ms. It can be seen that the operating time is slightly increased by increasing the fault resistance. The new protection has the ability to detect the internal fault even if the fault resistance is up to 600 Ω. The test results show that the average energies of two methods for an external fault are almost identical. The comparison shows that the new method is clearly superior, in terms of action speed or sensitivity and security, to the adaptive phasor based differential criterion.

5. Conclusions

The following conclusions can be conducted from the results of this paper:

- In the proposed protection, two different methods are applied to calculate the net energy fed into the protected line during a short time interval. The first method is to calculate the energy flow in a transmission line in a short time interval. The second method is to calculate the energy consumption of distributed elements on the transmission line with the assumption that there is no internal fault on the line.

- Four special means have been presented in Section 3. Then the energy of the two different methods can be calculated by using the sampled values of the voltage and current at each end of the transmission line.
- The energies of the two different methods are equal when there is no internal fault on the transmission line, which is proven in Appendix A.
- The proposed technique has highly reliability, fast speed, and excellent performance under high-resistance earth-fault conditions. The performance of the proposed method has been verified by EMTP simulation tests, dynamic simulation tests and the comparison with a competitive method.

Acknowledgment

This work was supported by the National Natural Science Foundation of China (51077061 and 50837002).

Appendix A

Substituting (5)–(8) into (10), $E_{1m1}(k)$ can be obtained as:

$$\begin{aligned}E_{1m1}(k) &= \int_{t_0+(k-1)\tau}^{t_0+k\tau}[v_{Mm1}(t)\cdot i_{Mm1}(t) - v_{Nm1}(t)\cdot i_{Nm1}(t)]dt \\ &= [2\cdot v_{Mm1}(k)\cdot i_{Mm1}(k) + 2\cdot v_{Mm1}(k-1)\cdot i_{Mm1}(k-1) \\ &\quad + v_{Mm1}(k)\cdot i_{Mm1}(k-1) + v_{Mm1}(k-1)\cdot i_{Mm1}(k)] \\ &\quad \cdot \tau/6 - [2\cdot v_{Nm1}(k)\cdot i_{Nm1}(k) + 2\cdot v_{Nm1}(k-1) \\ &\quad \cdot i_{Nm1}(k-1) + v_{Nm1}(k)\cdot i_{Nm1}(k-1) + v_{Nm1}(k-1) \\ &\quad \cdot i_{Nm1}(k)]\cdot \tau/6 \end{aligned} \tag{A1}$$

Substituting (3)–(8) into (11), $E_{2m1}(k)$ can be obtained as:

$$\begin{aligned}E_{2m1}(k) &= \int_{t_0+(k-1)\tau}^{t_0+k\tau}\int_0^l \left(i_{m1}^2(x,t)\cdot R_{m1} + i_{m1}(x,t)\cdot\frac{di_{m1}(x,t)}{dt}\right. \\ &\quad \left.\cdot L_{m1} + v_{m1}(x,t)\cdot\frac{dv_{m1}(x,t)}{dt}\cdot C_{m1}\right)dxdt \\ &= [A^2/9 + A\cdot A_M/3 + A\cdot A_{MN}/3 - A\cdot i_{Mm1}(k-1)/2 \\ &\quad + A_M^2/3 + A_M\cdot A_{MN}/2 - A_M\cdot i_{Mm1}(k-1) + A_{MN}^2/3 \\ &\quad - A_{MN}\cdot i_{Mm1}(k-1) - i_{Mm1}(k-1)\cdot i_{Mm1}(k-1)] \\ &\quad \cdot R_{m1}\cdot\tau + \{2\cdot[i_{Mm1}(k) + i_{Mm1}(k-1)][i_{Mm1}(k) \\ &\quad - i_{Mm1}(k-1)] + 2\cdot[i_{Nm1}(k) + i_{Nm1}(k-1)][i_{Nm1}(k) \\ &\quad - i_{Nm1}(k-1)] + [i_{Mm1}(k) + i_{Mm1}(k-1)][i_{Nm1}(k) \\ &\quad - i_{Nm1}(k-1)] + [i_{Nm1}(k) + i_{Nm1}(k-1)][i_{Mm1}(k) \\ &\quad - i_{Mm1}(k-1)]\}\cdot L_{m1}\cdot l/12 + \{2\cdot[v_{Mm1}(k) \\ &\quad + v_{Mm1}(k-1)][v_{Mm1}(k) - v_{Mm1}(k-1)] + 2 \\ &\quad \cdot[v_{Nm1}(k) + v_{Nm1}(k-1)][v_{Nm1}(k) - v_{Nm1}(k-1)] \\ &\quad + [v_{Mm1}(k) + v_{Mm1}(k-1)][v_{Nm1}(k) - v_{Nm1}(k-1)] \\ &\quad + [v_{Nm1}(k) + v_{Nm1}(k-1)][v_{Mm1}(k) - v_{Mm1}(k-1)]\} \\ &\quad \cdot C_{m1}\cdot\frac{l}{12} \end{aligned} \tag{A2}$$

where,

$$A = i_{Mm1}(k) - i_{Mm1}(k-1) - i_{Nm1}(k) + i_{Mm1}(k-1);$$

$$A_M = -i_{Mm1}(k) + i_{Mm1}(k-1);$$

$$A_{MN} = i_{Mm1}(k-1) - i_{Nm1}(k-1).$$

The partial differential equations of the single homogeneous transmission line are given by:

$$\frac{\partial v_{m1}(x,t)}{\partial x} = -L_0\frac{\partial i_{m1}(x,t)}{\partial t} - R_0 i_{m1}(x,t) \tag{A3}$$

$$\frac{\partial i_{m1}(x,t)}{\partial x} = -C_0\frac{\partial v_{m1}(x,t)}{\partial t}$$

If ignoring the line loss, the general solutions should be

$$\begin{cases} v_{m1}(x,t) = f_1(x-\upsilon t) + f_2(x+\upsilon t) \\ i_{m1}(x,t) = f_1(x-\upsilon t)/Z_C - f_2(x+\upsilon t)/Z_C \end{cases}$$

where x is the distance from a certain point to the relay position; υ the velocity of traveling wave, $\upsilon = 1/\sqrt{L_{m1}C_{m1}}$; t the time variable and Z_C is the wave impedance, $Z_C = \sqrt{L_{m1}/C_{m1}}$.

If $t_0 + (k-1)\tau$ is denoted as t, then $t + \tau = t_0 + k\tau$. The sampled values of the voltage and current at each end of the transmission line can be expressed as:

$$v_{Mm1}(k-1) = v_{m1}(0,t); \quad i_{Mm1}(k-1) = i_{m1}(0,t); \tag{A5}$$

$$v_{Mm1}(k) = v_{m1}(0,t+\tau); \quad i_{Mm1}(k) = i_{m1}(0,t+\tau);$$

$$v_{Nm1}(k-1) = v_{m1}(l,t); \quad i_{Nm1}(k-1) = i_{m1}(l,t);$$

$$v_{Nm1}(k) = v_{m1}(l,t+\tau); \quad i_{Nm1}(k) = i_{m1}(l,t+\tau).$$

Substituting (A4) and (A5) into (A1) and (A2), we can conclude that equation (A1) is equal to (A2), that is $E_{1m1}(k) = E_{2m1}(k)$. Thus it has been proven that the energies of the two different methods are equal when there is no internal fault on the transmission line.

References

[1] Tian Yu, Chunju Fan, Gong Zhendong. A study on accurate fault location algorithm for parallel transmission line with a teed connection. Int J Electr Power Energy Syst 2010;32(6):697–703.
[2] Abdul Gafoor Shaik, Ramana Rao Pulipaka V. A transient current based busbar protection scheme using wavelet transforms. Int J Electr Power Energy Syst 2011;33(4):1049–53.
[3] Bakar AHA, Mokhlis H, Illias HA, Chong PL. The study of directional overcurrent relay and directional earth-fault protection application for 33 kV underground cable system in Malaysia. Int J Electr Power Energy Syst 2012;40(1):113–9.
[4] Samantaray SR, Tripathy LN, Dash PK. Differential energy based relaying for thyristor controlled series compensated line. Int J Electr Power Energy Syst 2012;43(1):621–9.
[5] Eissa MM. A new digital busbar protection technique based on frequency information during CT saturation. Int J Electr Power Energy Syst 2013;45(1):42–9.
[6] Darwish HA, Taalab A-MI, Ahmed ES. Investigation of power differential concept for line protection. IEEE Trans Power Del 2005;20(2):617–24.
[7] Lin X, Tian Q, Zhao M. Comparative analysis on current percentage differential protections using a novel reliability evaluation criterion. IEEE Trans Power Del 2006;21(1):66–72.
[8] Aggarwal RK, Johns AT. A differential line protection scheme for power systems based on composite voltage and current measurements. IEEE Trans Power Del 1989;4(3):1595–601.
[9] Xu ZY, Du ZQ, Ran L, Wu YK, Yang QX, He JL. A current differential relay for a 1000-kV UHV transmission line. IEEE Trans Power Del 2007;22(3):1392–9.
[10] Jiang JA, Liu CW, Chen CS. A novel adaptive PMU-based transmission line relay—design and EMTP simulation results. IEEE Trans Power Del 2002;17(4):930–7.
[11] Xia Jingde, Jiale Suonan, Song Guobing, Wang Li, He Shien, Liu Kai. Transmission line individual phase impedance and related pilot protection. Int J Electr Power Energy Syst 2011;33(9):1563–71.
[12] Miao Shihong, Liu Pei, Lin Xiangning. An adaptive operating characteristic to improve the operation stability of percentage differential protection. IEEE Trans Power Del 2010;25(3):1410–7.
[13] Kawady Tamer A, Taalab Abdel-Maksoud I, Ahmed Eman S. Dynamic performance of the power differential relay for transmission line protection. Int J Electr Power Energy Syst 2010;32(5):390–7.